

# Ehime TORUS Model (e-torus) Users Manual

Version. 2016.05.06

Hisamitsu Awaki  
(awaki@astro.phys.sci.ehime-u.ac.jp)

---

## 1. Introduction

Compton-thick AGNs are suitable for the study of the reprocessed emission in AGNs, since their reprocessed emission dominates over the direct emission below 10 keV due to large column density  $N_{\text{H}} > 10^{24} \text{ cm}^{-2}$ . The baseline model based on previous observations worked well for reproducing the X-ray spectra of Compton-thick AGNs (e.g., Magdziarz & Zdziarski 1995; Cappi et al. 1999), and has contributed to our understanding of AGN. However, it is difficult to obtain information about the structure of the surrounding material from spectral fitting with this baseline model because the reflection model was developed for an accretion disk geometry. Thus, the reflection model does not match exactly with the actual reflection from the material around the black hole. Therefore, we need a model that represents X-ray emission from the surrounding material.

X-ray spectral models that describe the reprocessing of X-rays in a torus-shaped medium have been published. In “My Torus Model” by Murphy & Yaqoob 2009, they assume a doughnut-shaped torus geometry (see Fig. 1). Their model has been calculated for a single half-opening angle of  $60^\circ$  and is valid for column densities in the range  $10^{22}$  and  $10^{25} \text{ cm}^{-2}$ . “TORUS” Model calculated by Brightman & Nandra 2011 has the toroidal distribution of matter (Fig. 2). The parameters of the models are the line of sight column density of the neutral material ( $10^{20} \leq N_{\text{H}} \leq 10^{26} \text{ cm}^{-2}$ ) and the photon index of the intrinsic power law ( $1 \leq \Gamma \leq 3$ ). The opening angle of the torus ( $25.8^\circ \leq \theta_{\text{tor}} \leq 84.3^\circ$ ) and the inclination angle of the torus ( $18.2^\circ \leq \theta_i \leq 87.1^\circ$ ) are included. This model has validity in an energy range of 0.1 to 320 keV.

In our model, e-torus model, based on Ikeda et al. 2009, we assumed surrounding material with a three-dimensional torus configuration (Fig. 3) and simulated a spectrum from an AGN, considering the effect of Compton scattering and absorption. The intrinsic spectrum of AGN was described in the power law model with an exponential cut-off in the high-energy region. The opening angle ( $10^\circ \leq \theta_{\text{oa}} \leq 70^\circ$ ) and the equatorial column density ( $10^{22} \leq N_{\text{H}} \leq 10^{25} \text{ cm}^{-2}$ ) of the torus are considered in our simulation. In this

document, we present a brief explanation of our simulation and usage of the torus table model in XSPEC.

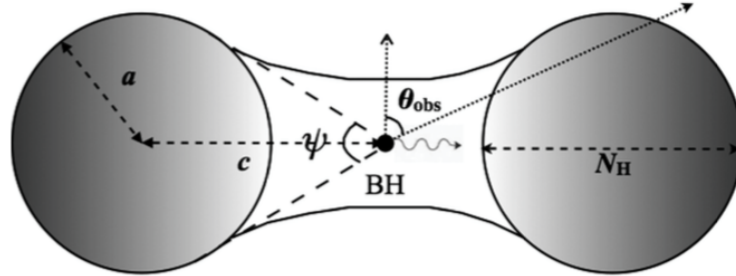


**Figure 1.** Assumed model geometry. The half-opening angle is given by  $(\pi - \psi)/2$  and the inclination angle of the observer's line of sight with the symmetry axis of the torus is given by  $\theta_{\text{obs}}$ . The equatorial column density,  $N_{\text{H}}$ , of the torus is defined by the diameter of the tube of the 'doughnut'.

Figure 1 “My torus model” by Murphy and Yaqoob 2009

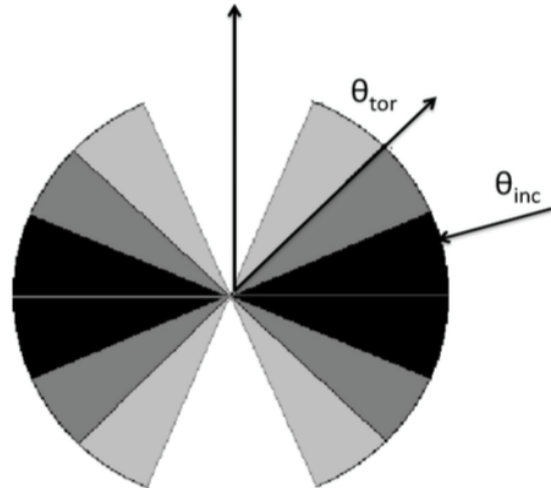


**Figure 1.** Geometry of the biconical torus distribution of matter used. The shading only serves to differentiate the different opening angles used, and does not correspond to density.

Figure 2 “TORUS” model by Brightman and Nandra 2011.

## 2. Model Definition

### 2.1 Basic assumptions

Surrounding material is assumed to be neutral and cold ( $T < 10^6$  K).

Metal abundance : cosmic abundance by Anders and Grevesse (1989)

Physical process :

Photoelectric absorption cross-section : Verner et al. (1996)

Compton scattering cross section : Klein-Nishina formula

Fe fluorescence line is only included.

Fluorescence yield: 0.34 (Bambynek et al. 1972)

$K\alpha$  and  $K\beta$  line transition probabilities: 150:17 (Kikoin 1976)

## 2.2 Geometry of the surrounding matter

Surrounding matter has a torus geometry shown in figure 3. The structure of the obscuring torus is characterized by the half-opening angle  $\theta_{oa}$ , the column density  $N_H$  along the equatorial plane, and the ratio of  $r_{in}$  to  $r_{out}$ . The primary X-ray source is located at the center of the torus. The inclination angle of the torus from an observer is  $\theta$ , .

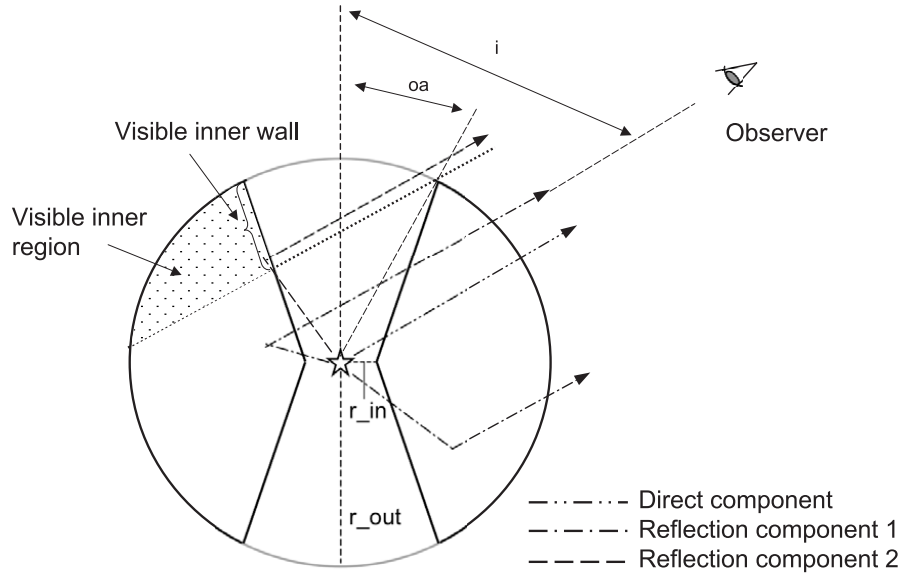


Figure 3. Cross-section view of the torus structure (Ikeda et al. 2009)

## 2.3 X-ray spectrum of the central engine

The primary X-ray source was assumed to emit photons with the energy spectrum  $I(E)$ .

$$I(E) \propto E^{-\Gamma} \exp(-E/Ec)$$

$\Gamma$ : photon index,  $Ec$ : cut off energy

Although our table model covers an energy range from 1 to 100 keV, we generated incident photons upto 1000 keV in our simulation, because the photons lose their energy due to Compton-down scattering. Figure 4 demonstrates the effect of the Compton down scattering in our torus model. In figure 4, each dot presents the photon energies before and after Compton scattering. The blue dotted line indicates the lowest energy of one Compton scattered photon ( $E=E/(1+2E/m_e c^2)$ ). Due to multiple scattering, the energies of some reflection photons are lower than the blue dotted line.

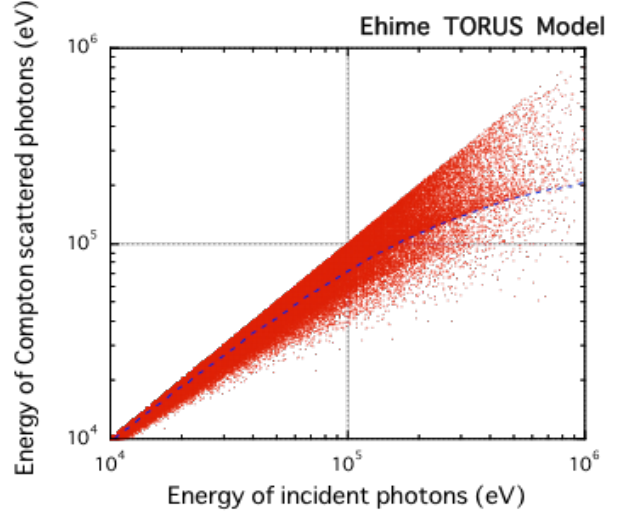


Figure 4 Effect of Compton Down Scattering

### 3. Simulation Parameters

Figure 5 is an example of a simulated AGN spectrum with  $N_H = 10^{24} \text{ cm}^{-2}$ ,  $\theta_{\text{oa}} = 40^\circ$ , and  $\theta_i = 45^\circ$ . The simulated spectrum is divided into three components for studying a dependence of the simulated spectrum on the torus geometry (Ikeda et al. 2009). Based on their study and an accuracy of the linear interpolation in XSPEC (see Appendix 1), we have determined the parameter grids of  $\theta_{\text{oa}}$  and  $N_H$  as follows,

$\theta_{\text{oa}}$  : 10 15 20 25 30 35 40 45 50 55 60 65 70  
 $r_{\text{in}}/r_{\text{out}}$  : 0.01 (fixed)  
 $N_H$  ( $\times 10^{22}$ ) : 1 3 5 7 10 30 50 70 100 200  
 300 400 500 700 1000

We considered 13 x 15 variations of the torus in our simulation. A torus was illuminated by X-ray emission from the central engine, which has a cut-off

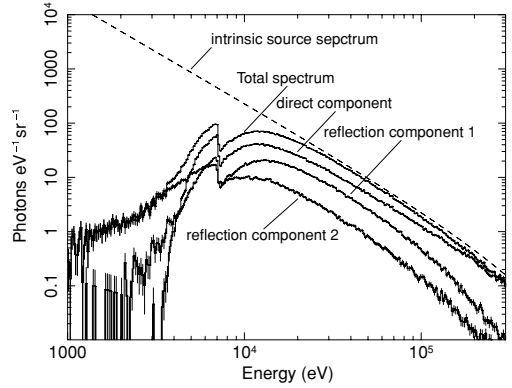


Figure 5 Example of our simulated AGN spectrum with  $N_H=10^{24} \text{ cm}^{-2}$ ,  $\theta_{\text{oa}}=40^\circ$ , and  $\theta_i=45^\circ$ . The simulated spectrum is divided into three components: the direct component, the reflection component 1, and the reflection component 2 as shown in this figure. The dashed line displays the intrinsic source spectrum. (original: figure 3 in Ikeda et al. 2009)

power-law emission as described in subsection 2.1. In case (1),  $E_c$  is fixed and  $\Gamma$  is varied from 1.5 to 2.5, while in case (2),  $\Gamma$  is fixed and  $E_c$  is varied from 20 to 500 keV.

(1)  $\Gamma = 1.5, 1.7, 1.9, 2.1, 2.3$  or  $2.5$ , and  $E_c = 360$  keV (fixed).

(2)  $\Gamma = 1.9$  (fixed), and  $E_c = 20, 50, 100, 200, 360$ , or  $500$  keV.

In total, we have simulated 2340 cases (=  $2 \times 6 \times 13 \times 15$  cases). Table 1 is a summary of the parameter grids.

Table 1 Summary of the parameter grid

	Parameters	Parameter grids
Torus	$\theta_{0a}$	10 15 20 25 30 35 40 45 50 55 60 65 70
	$N_H$	1 3 5 7 10 30 50 70 100 200 300 400 500 700 1000
Spectrum	(1)	$\Gamma=1.5, 1.7, 1.9, 2.1, 2.3, 2.5$ $E_c=360$ keV (fixed)
	(2)	$\Gamma=1.9$ (fixed) $E_c=20, 50, 100, 200, 360, 500$ keV

## 4. Results

We generated 2500M photons with a given spectrum. Each photon from the primary source had both an initial energy and an initial direction of propagation. If a photon was injected into the torus, an interaction point of the photon was calculated by using a random number. The photon was tracked until it escaped the torus structure, or until it was absorbed in the torus. The information of all escaped X-rays was stored in a file named “photon list”. Then, we extracted photons whose zenith angles of propagation ranged within  $\theta_{\pm 1^\circ}$  from the photon list. The extracted photons were accumulated into energy bins to form a spectrum. The accumulated spectrum is divided into three components : a direct component, a reflection component, and Fe line component consisting of Fe  $K\alpha$  and  $K\beta$  lines, where the direct component has no interaction with the surrounding material, while the reflection component consists of X-ray photons reflected in the surrounding material. Fe line component includes Compton shoulder.

### 4.1 Direct component

It is expected that the direct component is affected only by the column

density ( $N_{\text{is}}$ ) along our line of sight. We compared the simulated direct components with the cutoff power-law models, which were affected by both photoelectric absorption and Compton scattering. It is found that the models were in good agreement with the simulated direct components (see Ikeda et al. 2009). Thus, the model including the effect of Compton scattering is used instead of the simulated data for reproducing the direct component (5.2 (1)).

#### 4.2 Reflection component

Since the reflection component is so complex that we cannot make a simple model function, we reproduce this component by using a table model, covering the ranges of the photon index of 1.5–2.5,  $N_{\text{H}}$  of  $10^{22}$ – $10^{25}$   $\text{cm}^{-2}$ ,  $\theta_{\text{oa}}$  of  $10^\circ$ – $70^\circ$ , and  $\theta_{\text{i}}$  of  $0^\circ$ – $90^\circ$ . In order to reduce a dependency on the incident X-ray spectrum, the table model is given by the ratio of the reflection spectrum to the incident spectrum. Thus, the table model belongs to “multiplicative models”. The flag of the interpolation method for each parameter is set to 0 (linear). This is a structure of the table model, e-torus\_20160328\_2500M.fits, which is described in a FITS format (OGIP92).

Note: the reflection component in a spherical geometry with a given column density is obtained, if  $\theta_{\text{oa}} = 0$ .

#### **e-torus 20160329 2500M.fits**

No.	Type	EXTNAME	BITPIX Dimensions(columns)		PCOUNT	GCOUNT
0	PRIMARY		16	0	0	1
1	BINTABLE PARAMETERS		8	232(11) 4	0	1
	Column Name		Format	Dims	Units	TLMIN TLMAX
	1 NAME		12A			
	2 METHOD		J			
	3 INITIAL		E			
	4 DELTA		E			
	5 MINIMUM		E			
	6 BOTTOM		E			
	7 TOP		E			
	8 MAXIMUM		E			
	9 NUMBVALS		J			
	10 VALUE		45E			
	11 UNITS		8A			
2	BINTABLE ENERGIES		8	8(2) 960	0	1
	Column Name		Format	Dims	Units	TLMIN TLMAX
	1 ENERG_LO		E		keV	

2	ENERG_HI	E		keV		
3	BINTABLE SPECTRA	8	3856(2) 56700		0	1
	Column Name	Format	Dims	Units	TLMIN	TLMAX
	1 PARAMVAL	4E				
	2 INTPSPEC	960E		photons/cm^2/s		

## 5. Usage of “e-torus” model.

### 5.1 Preparation

#### (1) Download the package

The package can be picked up from the web site.

<http://heasarc.gsfc.nasa.gov/docs/xanadu/xspec/newmodels.html>

The package includes the latest version of “e-torus” model

torus\_model\_v02a.pdf (this document)  
e-torus\_20160329\_2500M.fits  
e-torus\_20160325\_hec\_2500M.fits

### 5.2 Reproduce the emission from a torus.

#### (1) direct component

To include the attenuation by Compton scattering, you can multiply the model *cabs* in your component as follows,

*phabs \* cabs \* cutoffpl* -- example 5-(a)

note: the column density of *cabs* (Compton scattering) should be linked to that of *phabs* (photoabsorption).

#### (2) reflection component by cold surrounding material

Ex. 5-(b) is an example of the reflection spectrum of e-torus model, when we assume that central source has a cut-off power law emission with a fixed cut-off energy of 360 keV. The table model belongs to “multiplicative models”. Therefore, **the photon index in the mtable model must be linked to that of cutoffpl**. If you want to change the cut-off energy, you can use the table model “e-torus\_20160325\_hec\_2500M.fits” instead of “e-torus\_20160329\_2500M.fits”. Please note that **the cut off energy in the mtable model must be linked to that of cutoffpl**.

*mtable{ e-torus\_20160329\_2500M.fits }\* cutoffpl* --- ex. 5-(b)



### (3) Iron line component

in preparation. Please wait for a moment.

## 6. Example

### 6.1 a simple case 1 --- nearly face on ( $N_{\text{is}} = 0$ )

The central engine is observed through an open area of a torus, i.e.  $\theta_1 < \theta_{\text{oa}}$ .

Thus, the column density  $N_{\text{is}}$  along our line of sight is expected to be 0.

#### (1) Define the model

```
XSPEC12>model cutoffpl + mtable{e-torus_20160329_2500M.fits}*cutoffpl
```

#### (2) Link and freeze the parameters

You must link the parameters of the spectral models for both the central X-ray source and the primary X-ray source to illuminate the torus. Furthermore, you must freeze *HighECut* in using the table model, e-torus\_20160329\_2500M.fits. If you use the table model e-torus\_20160325\_hec\_2500M.fits, you must freeze *PhoIndex*.

#### e-torus\_20160329\_2500M.fits

```
=====
```

Model	Model	Component	Parameter	Unit	Value	
par	comp					
1	1	cutoffpl	PhoIndex		1.90000	+/- 0.0
2	1	cutoffpl	HighECut	keV	360.000	frozen
3	1	cutoffpl	norm		0.100000	+/- 0.0
4	2	e-torus	nH	10^22	100.000	+/- 0.0
5	2	e-torus	PhoIn		1.90000	= 1
6	2	e-torus	Open_Ang	deg	30.0000	+/- 0.0
7	2	e-torus	Incl_Ang	deg	20.0000	+/- 0.0
8	2	e-torus	z		0.0	frozen
9	3	cutoffpl	PhoIndex		1.90000	= 5
10	3	cutoffpl	HighECut	keV	360.000	= 2
11	3	cutoffpl	norm		0.100000	= 3

---

**e-torus\_20160325\_hec\_2500M.fits**

Model cutoffpl<1> + mtable{ e-torus\_20160325\_hec\_2500M.fits}<2>\*cutoffpl<3> Source No.:

1 Active/Off

Model	Model Component	Parameter	Unit	Value
par	comp			
1	1	cutoffpl	PhoIndex	1.90000 frozen
2	1	cutoffpl	HighECut	keV 360.000 +/- 0.0
3	1	cutoffpl	norm	0.100000 +/- 0.0
4	2	e-torus	nH	10^22 100.000 +/- 0.0
5	2	e-torus	E_Cut	keV 360.000 = 2
6	2	e-torus	Open_Ang	deg 30.0000 +/- 0.0
7	2	e-torus	Incl_Ang	deg 10.0000 +/- 0.0
8	2	e-torus	z	0.0 frozen
9	3	cutoffpl	PhoIndex	1.90000 = 1
10	3	cutoffpl	HighECut	keV 360.000 = 2
11	3	cutoffpl	norm	0.100000 = 3

Figure 6 shows the model spectrum. The direct and the reflection components are presented by *cutoffpl<1>* and *mtable<2>\*cutoffpl<3>*, respectively. *Cutoffpl<3>* is considered to be the primary source to illuminate the torus. If the central source shows a time variability, you may release the link of normalizations of *cutoffpl <1>* and *cutoffpl <3>* due to a time lag between the direct light and reflection light.

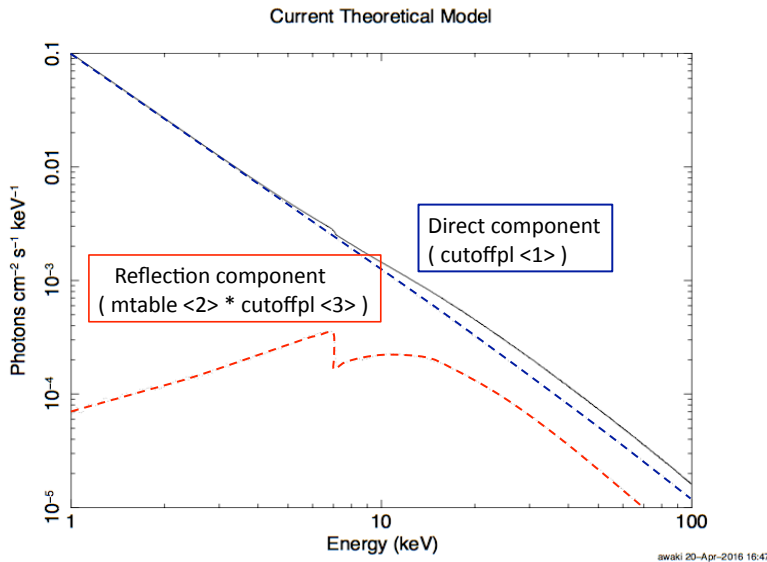


Figure 6. A model spectrum in a simple case 1.

Blue and red lines show the direct and reflection components, respectively.

6.2 a simple case2 -----  $N_{\text{ls}}/N_{\text{eq}} \sim 1$ .

From the geometry of our torus model (figure 3), the ratio of  $N_{\text{ls}}/N_{\text{eq}}$  is expressed as a function of the inclination angle  $\theta_i$ . In the case of  $\theta_i > \theta_{\text{oa}} + 5^\circ$ , you may assume  $N_{\text{ls}}/N_{\text{eq}} \sim 1$ .

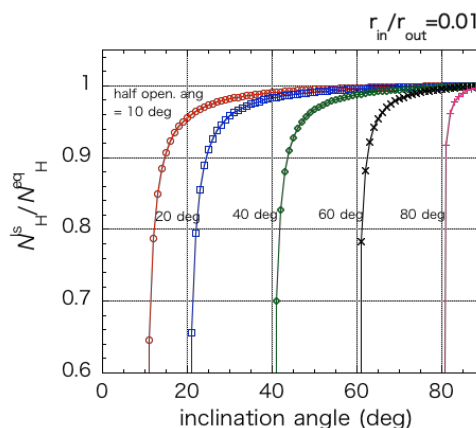


Figure 7  $N_{\text{ls}}/N_{\text{eq}}$  as a function of inclination angle  $\theta_i$ .

(1) define the model

```
XSPEC12>model
```

```
phabs*cabs*cutoffpl+mtable{refl_all_20160329_2500M.fits}*cutoffpl
```

(2) link and freeze the parameters

After define the spectral model, you should link the parameters of the spectral models for both the central X-ray source and the primary X-ray source, and freeze *HighECut*. This is an example. The model spectrum is shown in figure 8.

**e-torus\_20160329\_2500M.fits**

```
Model phabs<1>*cabs<2>*cutoffpl<3> + mtable{ e-torus_20160329_2500M.fits}<4>*cutoffpl<5>
Source No.: 1 Active/Off
```

Model par	Model comp	Component	Parameter	Unit	Value	
1	1	phabs	nH	10 <sup>22</sup>	100.000	+/- 0.0
2	2	cabs	nh	10 <sup>22</sup>	100.000	= 1
3	3	cutoffpl	PhoIndex		1.90000	+/- 0.0
4	3	cutoffpl	HighECut	keV	360.000	frozen
5	3	cutoffpl	norm		0.100000	+/- 0.0
6	4	e-torus	nH	10 <sup>22</sup>	100.000	= 1
7	4	e-torus	PhoIn		1.90000	= 3
8	4	e-torus	Open_Ang	deg	30.0000	+/- 0.0
9	4	e-torus	Incl_Ang	deg	50.0000	+/- 0.0
10	4	e-torus	z		0.0	frozen
11	5	cutoffpl	PhoIndex		1.90000	= 3
12	5	cutoffpl	HighECut	keV	360.000	= 4
13	5	cutoffpl	norm		0.100000	= 5

The heavily absorbed direct component is expressed as  $phabs<1>*cabs<2>*cutoffpl<3>$ , while the reflection component is presented by  $mtable<4>*cutoffpl<5>$ . You may release the link of normalizations of  $cutoffpl<3>$  and  $cutoffpl<5>$  to examine a time variability of the central X-ray source.

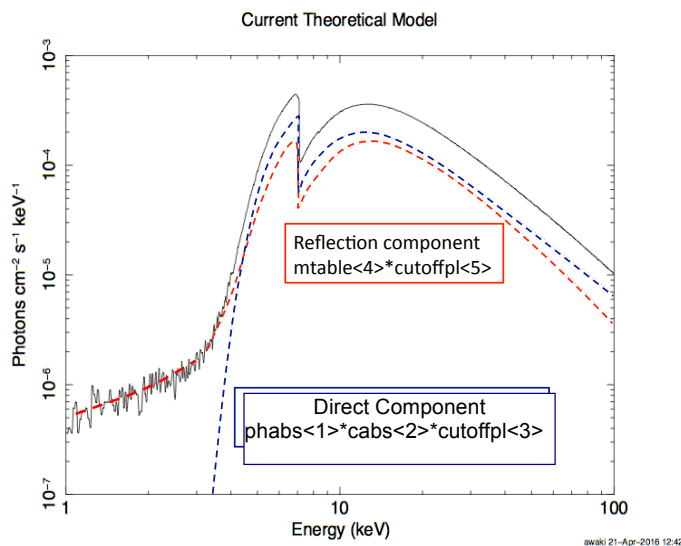


Figure 8. A model spectrum in a simple case 2.

Blue and red lines show the direct and reflection components, respectively.

### 6.3 Advanced application

In the case of  $\theta_l \sim \theta_{0a}$ , the column density  $N_{ls}$  may be different from the column density  $N_{eq}$ . Furthermore, the torus may contain clumpy clouds, and we may observe the central source through the optically thick clumpy clouds.

To meet your requirement, you can delink the parameters  $N_{ls}$  and  $N_{eq}$ . In addition, you can use independent normalizations of the direct and reflection components.

### 6.4 Note on $\theta_{0a}$ and normalization of the reflection component.

The quality of an observed spectrum is not good,  $\theta_{0a}$  may be coupled with normalization of the reflection component, because the reflection matter depends on  $\theta_{0a}$ . Ikeda et al. (2009) demonstrates this dependency in fitting the Suzaku wide-band spectrum of Mrk 3.

## 7 Error estimation

We recommend to use “*steppar*” command to estimation an error of  $\theta_{\text{oa}}$  or  $\theta_i$ , because in using “*steppar*” command, we can adjust the step of the parameter to the parameter grid. This is an example in the simple case 2.

```
steppar 8 20.0 40.0 4
```

“*Steppar*” command search the confidence region of parameter 8 ( $\theta_{\text{oa}}$ ) in the region of 20.0-40.0 degree with a step of 5 degree ( $\theta_{\text{oa}} = 20.0, 25.0, 30.0, 35.0, 40.0$ ). Another example is

```
steppar 9 31 41 5
```

The stepping value is equal to the grid of  $\theta_i$  ( 31, 33, 35,37,39, and 41 ).

We note that if the confidence region of  $\theta_{\text{oa}}$  is not estimated well, we recommend that  $\theta_i$  links to  $\theta_{\text{oa}}$  as  $\theta_i = \theta_{\text{oa}} + \Delta$ . The  $\Delta$  is deduced from the best-fit value, which is rounded to the nearest integer.

## Acknowledgement

This work was supported by JSPS KAKENHI Grant Number 15H02070. HA wishes to thank Ms. Koike for her help.

## References

- E. Anders & N. Grevesse, *Geo.Cos. Acta.*, **197**, 214 (1989)
- W. Bambynek et al., *RvMP*, **44**, 716-813 (1972)
- M. Brightman and K. Nandra, *MNRAS*, **413**, 1206-1235 (2011)
- M. Cappi et al., *A&A*, **344**, 857-867 (1999)
- S. Ikeda, H. Awaki, and Y. Terashima, *ApJ*, **692**, 608-617 (2009)
- I. K. Kikoin, “Tables of Physical Quantities”, (1976)
- P. Magdziarz & A.A. Zdziarski, *MNRAS*, **273**, 837-848 (1995)
- K.D. Murphey and T. Yaqoob, *MNRAS*, **397**, 1549–1562 (2009)
- D.A. Verner et al., *ApJ*, **465**, 487 (1996)

[http://heasarc.gsfc.nasa.gov/docs/heasarc/ofwg/docs/general/ogip\\_92\\_009/ogip\\_92\\_09.html](http://heasarc.gsfc.nasa.gov/docs/heasarc/ofwg/docs/general/ogip_92_009/ogip_92_09.html)

## Appendix 1 Evaluation of the interpolation of XSPEC table model

